computational overestimation of the compression of the bond angles H(5)-C(5)-O(13) and H(9)-C(9)-Cl(9) and by the exaggerated calculated nonbonded distance C(5)···C(9) (Table II, Figure 2c). A similar pattern of deviations between experiment and calculations has been found previously for **1** and **2**.[4] The results of the neutron diffraction measurement on **8** therefore indicate again an excessive hardness at short distances of the nonbonded H···H potential used in the MM2 force field. On the other hand, it is noteworthy that the short Cl(9)···Cl(11a) distance of 3.042 Å calculated for **9** agrees well with the value of 3.048 (1) Å observed for **8** (Table II).

The severe H···H repulsions in the present fused norbornane compounds are also reflected through unusual increased C-H stretching (ν_{CH}) frequencies as has been found by Winstein et al.[22] more than 20 years ago. These frequency enhancements occur for those normal modes that involve simultaneous stretching and compression, respectively, of the inner congested C-H bonds.[5,22] In keeping with the extraordinarily short inner H···H distance, the largest measured (IR, KBr disk) ν_{CH} frequency of **8** has the very high value of 3119 cm^{-1} and may be assigned to synchronous inner C-H stretchings (methine ν_{CH} of 2-chloropropane for comparison, 2962 cm^{-1} [23]).[24] Expectedly, the largest ν_{CH} frequency of the less congested chlorine-free half-cage is smaller (IR value of **5**, 3048 cm^{-1} [22]), although still markedly enhanced as compared to the corresponding norbornane frequency (2950-2965 cm^{-1} [25]).[26,28d]

It is tempting to speculate about unusual chemical consequences of the close proximity of the inner congested hydrogen atoms in the present fused norbornane systems. Paquette et al. found that secododecahedrane **11** (and a methyl derivative), which involves

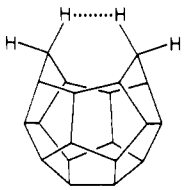

11

two topologically similar congested methylene groups (X-ray H···H distance of a dimethyl derivative, 1.95 (11) Å;[28b] calculated with the CFF, 1.884 Å[5]), may be catalytically dehydrogenated to form dodecahedrane under unusually mild conditions (Pd/C, 250 °C).[28a] It is conceivable that the fused norbornane compounds display a similar behavior although according to force field calculations the thermodynamic driving force for the replacement of the pair of congested hydrogen atoms by a C-C bond is expected to be smaller (lower strain release) than for secododecahedrane/dodecahedrane.

Acknowledgment. Financial support of the Fonds der Chemischen Industrie is gratefully acknowledged.

Registry No. 8, 95193-11-6.

Supplementary Material Available: Observed and calculated neutron structure amplitudes for **8** (14 pages). Ordering information is given on any current masthead page.

(22) Kivelson, D.; Winstein, S.; Bruck, P.; Hansen, R. L. *J. Am. Chem. Soc.* **1961**, *83*, 2938.
(23) McKean, D. C.; Saur, O.; Travert, J.; Lavalley, J. C. *Spectrochim. Acta, Part A* **1975**, 31*A*, 1713.
(24) In order to avoid any confusion that might arise from the aromatic ν_{CH} frequencies of **8**, the IR spectrum of the corresponding hexachloro half-cage propionate was recorded in addition (CCl_4 solution), which also shows a band at 3119 cm^{-1}.
(25) Meić, Z.; Randić, M.; Rubčić, A. *Croat. Chem. Acta* **1974**, *46*, 25. Brunel, Y.; Coulombeau, C.; Coulombeau, C.; Moutin, M.; Jobic, H. *J. Am. Chem. Soc.* **1983**, *105*, 6411.
(26) Similarly, the largest (enhanced) ν_{CH} frequency of the *exo,exo*-tetracyclododecane hydrocarbon underlying **1** (3052 cm^{-1} [22]) is smaller than that of the anhydride derivative **2** (3078 cm^{-1}; IR, KBr disk) whose inner H···H distance is shorter. It is noted that the CFF underestimates the ν_{CH} enhancements in this class of compounds since a simple harmonic C-H stretching function is used rather than a more realistic anharmonic potential, e.g., a Morse function.[5,27,28d] The present fused norbornane compounds also display enhanced δ_{CH_2} scissoring frequencies which involve simultaneous opening and compression, respectively, of the H-C-H angles of the inner congested methylene groups. The CFF overestimates these δ_{CH_2} enhancements considerably, mainly due to the excessive hardness of the nonbonded H···H potential used.[5,27,28d]
(27) Ermer, O.; Ivanov, P. M.; Ōsawa, E., manuscript in preparation.
(28) (a) Paquette, L. A.; Ternansky, R. J.; Balogh, D. W.; Kentgen, G. *J. Am. Chem. Soc.* **1983**, *105*, 5446. Paquette, L. A.; Ternansky, R. J.; Balogh, D. W.; Taylor, W. J. *Ibid.* **1983**, *105*, 5441. (b) Christoph, G. G.; Engel, P.; Usha, R.; Balogh, D. W.; Paquette, L. A. *Ibid.* **1982**, *104*, 784. (c) Paquette, L. A.; Balogh, D. W. *Ibid.* **1982**, *104*, 774. (d) It is noted that secododecahedrane **11** as well as a monomethyl- and a dimethylsecododecahedrane show enhanced ν_{CH} frequencies which are likely to arise from the H···H repulsions between the congested methylene groups and whose normal coordinates are characterized by synchronous stretchings of the inner methylene C-H bonds. However, the reported ν_{CH} frequencies of 3030,[28a] 3020,[28a] and 3150 cm^{-1},[28c] respectively, for these three cage molecules are not consistent. The frequency of 3150 cm^{-1} for the dimethyl derivative really appears *too* high; a printing error might have interfered and the correct value could be 3050 cm^{-1} (?). The CFF gives a calculated largest ν_{CH} frequency of 2985 cm^{-1} for secododecahedrane **11**,[5] again smaller than observed as in the case of the fused norbornane systems.[5,26]

Molecular Dynamics of a Peptide Chain, Studied by Intramolecular Excimer Formation

R. Goedeweeck, M. Van der Auweraer, and F. C. De Schryver*

Contribution from the Department of Chemistry, K. U. Leuven, Celestijnenlaan 200 F, B-3030 Heverlee, Belgium. *Received June 27, 1984*

Abstract: Both diastereomers of the dipeptide *N*-acetylbis(1-pyrenylalanine) methyl ester were studied by means of stationary and transient fluorescence measurements as model compounds of the random-coiled peptide chain. The diastereomeric differences and the solvent influences could be correlated with the populations of two sets of ground-state conformations: an extended conformation, unable to form an excimer, in equilibrium with a folded conformation which does allow a transition to the excimer geometry within the lifetime of an excited pyrene moiety. A consecutive kinetic scheme was used to calculate some relevant kinetic and thermodynamic parameters. Conformational populations have been calculated in toluene (high folded population) and ethyl acetate (high extended population). The conformational equilibrium of the threo diastereomer is shifted to the extended conformation, compared with the erythro diastereomer in the same solvent, because of the larger steric hindrance between the amino acid side groups in the threo folded conformation.

During several decades, the study of protein luminescence has been limited to the detection of the intrinsic fluorescence of the natural aromatic amino acids[1] or the extrinsic emission of artificial probes, adsorbed or bound covalently at the protein.[2] Often, a

0002-7863/85/1507-2334$01.50/0

protein fluorescence decay shows high complexity due to the nonexponential behavior of tryptophan, the presence of several fluorescent amino acids at different sites in the protein or multiple binding, or adsorption of probes. Moreover, natural proteins have low emission quantum yields.

More recently, the emission properties of the homopolymers of several aromatic amino acids have been studied, e.g., poly(naphthylalanine),[3] poly(pyrenylalanine),[4] aromatic esters of polyglutamate[5] and -aspartate,[6] and poly(phenylalanine).[7] These compounds are not subject to the disadvantages of natural proteins but their photophysics are characterized by phenomena such as ground-state interactions between adjacent chromophores, energy migration, deviating behavior of chromophores at the chain ends, intrachain interactions between chromophores, separated by several amino acid residues, and transitions of the secondary structure of the polymer (e.g., helix–coil transition). Besides, the solubility of such compounds is often extremely low.[4]

Similar difficulties are encountered when studying polyvinyl aromatic compounds. It could be shown, however, that the corresponding diastereomeric 2,4-diarylpentanes are adequate model compounds to describe the photophysics of these polymers.[8] Both pentanes reflect the conformational and configurational influence of the ground state on the process of excimer formation, thereby revealing important information on the molecular dynamics of the polymer.

Until now, no fluorescence study of dipeptides as model systems of the random-coiled peptide chain has been reported. In this paper, the molecular dynamics of both diastereomers of *N*-acetylbis(1-pyrenylalanine) methyl ester (BPA), probed by the excimer formation between both pyrenes, are discussed.

Experimental Section

Materials. The synthesis, purification, separation, and identification of e- and t-BPA and PA have been described before.[9] Most solvents (Merck Uvasol) were used without further purification, with the exception of the chlorinated alkanes and tetrahydrofuran which were refluxed over sodium and distilled. Acetone was purified and dried by passing over a column containing activated charcoal and silica gel. Ethyl acetate was purified from hydrolysis products by distilling under nitrogen atomosphere.

Measurements. The concentrations were kept lower than 10^{-5} M and all solutions were degassed by the freeze–pump–thaw technique (five cycles). Absorption spectra were recorded on a Perkin-Elmer 550S spectrophotometer and fluorescence spectra on a SPEX fluorolog (excitation at 343 nm). All emission spectra are corrected and the quantum yields were determined with reference to a solution of quinine sulfate in 1 N sulfuric acid and corrected for the refractive index of the solvent. Fluorescence decays were measured by means of the time-correlated single photon-counting technique which is described in photon-counting in ref 10. Excitation in ethyl acetate was performed at 300 nm with a frequency-doubled, cavity-dumped rhodamine-dye laser, synchronously pumped by a mode-locked argon laser (all instruments by Spectraphysics).

The maximum pulse width was 20 ps and the repetition rate was 400 kHz. Decays in toluene were obtained by excitation at 343 nm with a deuterium-filled flash lamp with a repetition rate of 14 kHz and a pulse width of about 2 ns. The instrumental response function was detected by measuring experimentally the excitation pulse shape or by means of the excitation pulse shape mimic technique with a xanthione[11] solution in isooctane, analyzed at 480 nm, and a benzo[*b*]indeno[1,2-*e*]pyran[12] solution in isooctane, analyzed at 377 nm. The electronic equipment was composed of Canberra and Ortec modules, and a typical measurement proceeded until at least 15 000 counts were collected in the maximum channel of the Canberra 8100 multichannel analyzer. The locally excited state of pyrene was analyzed at 377 nm and the excimer emission at 480 nm (Jobin–Yvon H10 double monochromator). All decays were deconvoluted on a PDP-11/23 computer.

Table I. Ratio of the Quantum Yield of Excimer Emission (ϕ_{exc}) and Emission from the Locally Excited State (ϕ_{py}) in Various Solvents, with Taft Parameters α, β, and π

solvent	ϕ_{exc}/ϕ_{py} e-BPA	ϕ_{exc}/ϕ_{py} t-BPA	α	β	π
dichloromethane	3.0	1.0	0.0	0.0	0.80
1,2-dichloroethane	3.1	1.0	0.0	0.0	0.81
benzene	2.3	1.1	0.0	0.10	0.59
ethyl acetate	1.0	0.29	0.0	0.48	0.55
diethyl ether	0.93	0.22	0.0	0.49	0.27
acetone	1.2	0.45	0.10	0.50	0.68
tetrahydrofuran	1.0	0.31	0.0	0.55	0.58
dimethylacetamide	0.50	0.17	0.0	0.75	0.88
butanol	2.3	0.68	0.79	0.88	0.46
ethanol	2.4	0.75	0.85	0.77	0.54
methanol	2.5	0.75	0.99	0.62	0.59
ethylene glycol	1.1	0.37	0.99	0.52	0.73
trifluoroethanol	8.4	2.9	1.66	0.0	1.02

Results

The structure of BPA and also the assignment of the prefixes "threo" (t) and "erythro" (e) to each diastereomer are shown below. In order to reduce the number of possible ground-state

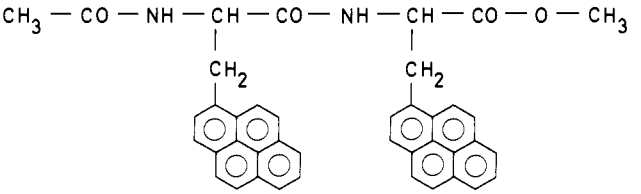

D,D and L,L : threo

D,L and L,D : erythro

conformations, the carboxylate end of the peptide chain was chosen to be an ester rather than an amide. In the latter case, folding to the β turn (also called the C_{10} conformation) becomes possible, and this subject was considered to be part of a separate project.

When compared with the spectrum of the reference compound, D,L-*N*-acetyl-1-pyrenylalanine methyl ester (PA), e- and t-BPA show a new bathochromic and structureless emission band, ascribed to the fluorescence of an intramolecular pyrene excimer with emission maxima at 465 nm (e-BPA) and 455 nm (t-BPA). Some representative spectra were published previously.[9] No significant differences in the absorption and excitation spectra of BPA and PA could be detected, indicating the absence of an interaction between the pyrenyl side groups in the ground state.

Table I lists the values of the ratio of the quantum yield of excimer emission ϕ_{exc} and the quantum yield of emission from the locally excited state ϕ_{py} in various types of solvents, each of which is characterized by three Taft parameters.[13] α is an index

(1) Review by: Eftink, M. R.; Ghiron, C. A. *Anal. Biochem.* **1981**, *114*, 199–227.
(2) Review by: Radda, G. K. *Biochem. J.* **1971**, *122*, 385–416.
(3) (a) Sisido, M.; Egusa, S.; Imanishi, Y. *J. Am. Chem. Soc.* **1983**, *105*, 1041–1049. (b) Sisido, M.; Egusa, S.; Imanishi, Y. *Ibid.* **1983**, *105*, 4077–4082.
(4) Egusa, S.; Sisido, M.; Imanishi, Y. *Chem. Lett.* **1983**, 1307.
(5) (a) Ueno, A.; Toda, F.; Iwakura, Y. *Biopolymers* **1974**, *13*, 1213–1222. (b) Ueno, A.; Osa, T.; Toda, F. *J. Polym. Sci., Polym. Lett. Ed.* **1976**, *14*, 521–529.
(6) (a) Ueno, A.; Ishigura, T.; Toda, F.; Uno, K.; Iwakura, Y. *Biopolymers* **1975**, *14*, 353–362. (b) Ueno, A.; Osa, T.; Toda, F. *Macromolecules* **1977**, *10*, 130–135.
(7) (a) Leroy, E.; Lapp, C. F.; Laustriat, G. *Biopolymers* **1974**, *13*, 507–522. (b) Lapp, C. F.; Laustriat, G. *J. Chim. Phys.* **1971**, *68*, 1333–1341.
(8) (a) De Schryver, F. C.; Demeyer, K.; Van der Auweraer, M.; Quanten, E. *Ann. N. Y. Acad. Sci.* **1981**, *366*, 93–108. (b) Ito, S.; Yamamoto, M.; Nishijima, Y. *Bull. Chem. Soc. Jp.* **1981**, *54*, 35–40. (c) De Schryver, F. C.; Vandendriessche, J.; Toppet, S.; Demeyer, K.; Boens, N. *Macromolecules* **1982**, *15*, 406–408. (d) Monnerie, L.; Bokobza, L.; De Schryver, F. C.; Moens, L.; Van der Auweraer, M.; Boens, N. *Ibid.* **1982**, *15*, 64–66. (e) Collart, P.; Demeyer, K.; Toppet, S.; De Schryver, F. C. *Ibid.* **1983**, *16*, 1390–1391.
(9) Goedeweeck, R.; De Schryver, F. C. *Photochem. Photobiol.* **1984**, *39*, 515–520.
(10) Boens, N; Van Den Zegel, M.; De Schryver, F. C. *Chem. Phys. Lett.* **1984**, *111*, 340–346.
(11) James, D. R.; Demmer, D. R. M.; Verall, R. E.; Steer, R. P. *Rev. Sci. Instrum.* **1983**, *54*, 1121–1130.
(12) Ware, W. R.; Pratinidhi, M.; Bauer R. K. *Rev. Sci. Instrum.* **1983**, *54*, 1148–1156.

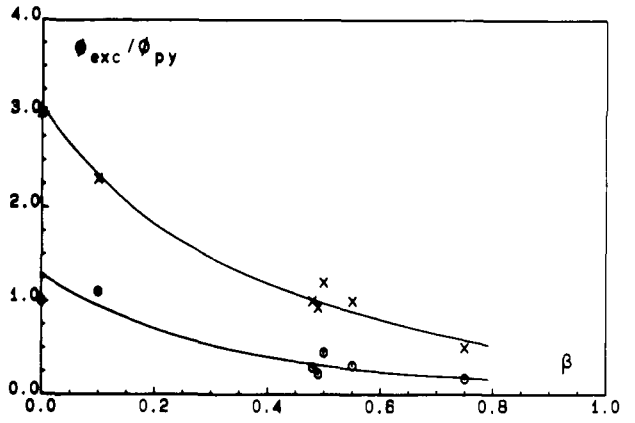

Figure 1. Ratio of the quantum yield of excimer emission ϕ_{exc} and emission from the locally excited state ϕ_{py} vs. the basicity Taft parameter of the hydrogen-accepting solvents (benzene, ethyl acetate, diethyl ether, acetone, tetrahydrofuran, and *N*,*N*-dimethylacetamide according to increasing value) and chloroform with $\beta = 0$: ×, e-BPA; ○, t-BPA.

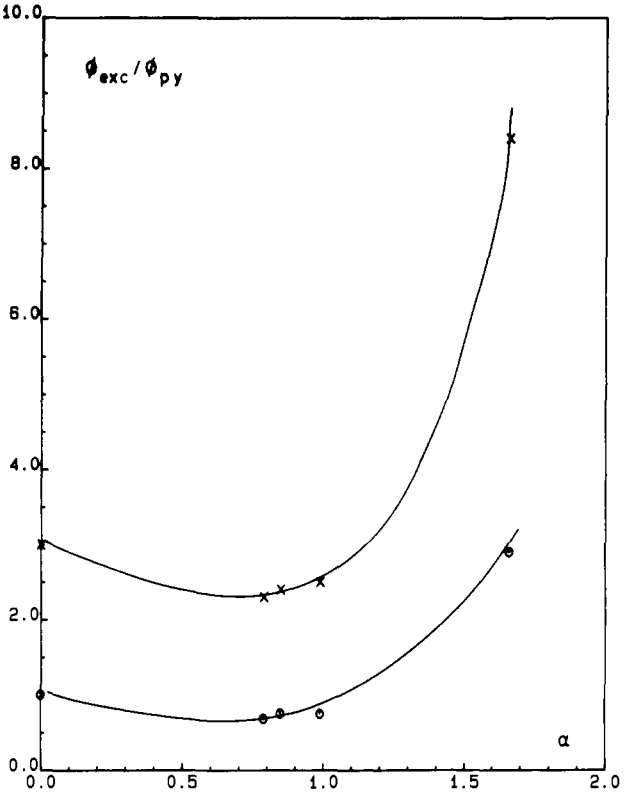

Figure 2. Ratio of the quantum yield of excimer emission ϕ_{exc} and emission from the locally excited state ϕ_{py} vs. the acidity Taft parameter of the alcohols (butanol, ethanol, methanol, and trifluoroethanol according to increasing value) and chloroform with $\alpha = 0$: ×, e-BPA; ○, t-BPA.

of solvent (hydrogen bond donor) acidity and β is an index of solvent (hydrogen bond acceptor) basicity. π is a measure of solvent polarity and polarizability. It is clear from the data in Table I that the value of ϕ_{exc}/ϕ_{py} is very dependent on the tendency of the solvent to interact with the peptide function by hydrogen bonding. Large values of ϕ_{exc}/ϕ_{py} are obtained in solvents with $\alpha = \beta = 0$, but the values decrease progressively with increasing hydrogen-accepting ability of the solvent (Figure 1). In weak

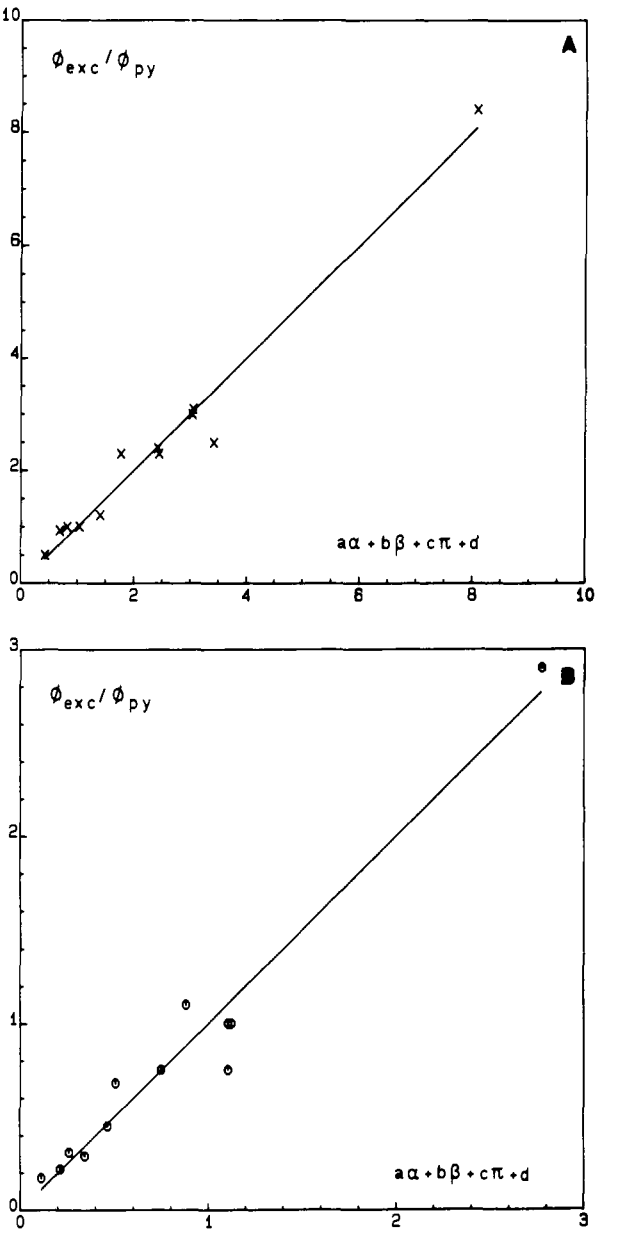

Figure 3. Ratio of the quantum yield of excimer emission ϕ_{exc} and emission from the locally excited state ϕ_{py} vs. the values calculated with the Taft function $a\alpha + b\beta + c\pi + d$. (A) e-BPA: $a = 2.880$, $b = -3.601$, $c = 1.113$, $d = 2.154$. (B) t-BPA: $a = 0.947$, $b = -1.372$, $c = 0.420$, $d = 0.770$.

alcohols also a lower value of ϕ_{exc}/ϕ_{py} is observed, but in very acidic solvents such as 2,2,2-trifluoroethanol, a very large ratio is obtained (Table I and Figure 2).

All solvents can be treated as one group, however, when fitting the values of the dependent variable ϕ_{exc}/ϕ_{py} with multiple linear regression to the independent variables α, β, and π (Figure 3). The autocorrelations between the ϕ_{exc}/ϕ_{py} ratio and the values calculated with the Taft functions $a\alpha + b\beta + c\pi + d$ are 0.985 and 0.978 for e- and t-BPA respectively.[14] The values of the calculated coefficients a, b, c, and d of both diastereomers are given in the caption of Figure 3. c, the coefficient of π, has in both cases a lower value than the coefficients a and b, indicating that the excimer formation in BPA is mainly influenced by hydrogen bonding with the solvent rather than by solvent polarity. The negative value of b illustrates the unfavorable effect of hydrogen-accepting solvent properties on the ϕ_{exc}/ϕ_{py} ratio, but the

(13) (a) Kamlet, M. J.; Taft, R. W. *J. Am. Chem. Soc.* **1976**, *98*, 377–383. (b) Taft, R. W.; Kamlet, M. J. *Ibid.* **1976**, *98*, 2886–2894. (c) Kamlet, M. J.; Abboud, J. L.; Taft, R. W. *Ibid.* **1977**, *99*, 6027–6038. (d) Abboud, J. L.; Taft, R. W. *J. Phys. Chem.* **1979**, *83*, 412–419. (e) Taft, R. W.; Gramstad, T.; Kamlet, M. J. *J. Org. Chem.* **1982**, *47*, 4557–4563. (f) Taft, R. W., Pienta, N. J.; Kamlet, M. J.; Arrett, E. M. *Ibid.* **1981**, *46*, 661–667. (g) Taft, R. W.; Kamlet, M. J. *J. Chem. Soc., Perkin Trans. 2* **1979**, 1723–1729.

(14) The low values obtained in ethylene glycol are not included in the calculations since this is mainly due to viscosity rather than hydrogen bond effects.

Table II. Decay Parameters of the Fast, λ_F, and Slow Decay, λ_S, Ratio of the Preexponentials A_F/A_S of the Locally Excited State of e- and t-BPA in Ethyl Acetate, and Lifetime of PA in Ethyl Acetate at Different Temperatures

	e-BPA			t-BPA			
temp (°C)	λ_F^{-1} (ns)	λ_S^{-1} (ns)	A_F/A_S	λ_F^{-1} (ns)	λ_S^{-1} (ns)	A_F/A_S	τ^0 (ns)
−70	87	226	0.28		268		276
−60	65	208	0.31	24	263	0.17	273
−50	51	185	0.29	21	249	0.22	270
−40	35	159	0.33	16	234	0.28	266
−30	30	137	0.32	14	214	0.31	261
−20	23	120	0.37	11	190	0.35	253

Table III. Decay Parameters of the Fast, λ_F, and the Slow Decay, λ_S, and Ratio of the Preexponentials A_F/A_S of the Locally Excited State of e- and t-BPA in Toluene, and Lifetime of PA in Toluene at Different Temperatures

	e-BPA			t-BPA			
temp (°C)	λ_F^{-1} (ns)	λ_S^{-1} (ns)	A_F/A_S	λ_F^{-1} (ns)	λ_S^{-1} (ns)	A_F/A_S	τ^0 (ns)
−80	124	225	1.79	30	230	0.22	235
−70	96	191	1.61	22	221	0.31	230
−60	77	174	1.43	15	200	0.40	229
−50	61	140	1.30	12	173	0.48	220
−40	45	114	1.21	9.5	149	0.56	212
−30	39	93	1.29	7.1	127	0.62	209
−20	28	76	1.03	5.1	108	0.67	208

positive value of a implies that acidic solvents facilitate the excimer formation. This explains the shape of the curve in Figure 2 showing the dual influence of alcohols, as they are amphoteric solvents. Alcohols with a low acidity induce smaller values of ϕ_{exc}/ϕ_{py} than solvents with $\alpha = \beta = 0$ because of their hydrogen-accepting properties. Very acidic alcohols, however, have negligible β but large α values, resulting in a very high ϕ_{exc}/ϕ_{py} ratio.

These solvent influences will be explained in the next section in terms of population changes of ground-state conformations of BPA. In all solvents studied, the values of ϕ_{exc}/ϕ_{py} are larger for e- than for t-BPA, reflecting the higher ability of the erythro diastereomer to adopt conformations which allow a transition to the excimer geometry within the lifetime of excited pyrenylalanine.

Two solvents were selected for quantitative measurements: toluene as a solvent inert toward hydrogen bonds and ethyl acetate as an hydrogen acceptor. Figure 4 shows the results of a stationary study of e- and t-BPA in ethyl acetate as a function of temperature. The deviation from the straight line in the low-temperature region of Figure 4 suggests that the repopulation of locally excited state from the excimer becomes possible from −20 °C for both diastereomers. This conclusion is supported by the single photon-counting analysis of e- and t-BPA in both solvents as function of temperature. Some representative decay curves are reported in Figure 5, and the experimental decay parameters and preexponential terms are listed in Tables II and III.

Below −20 °C a two-exponential decay of the locally excited state is observed, a component with decay parameters λ_S, decaying slowly, and a fast component with decay parameter λ_F. Above −20 °C, the time-dependent intensity of the locally excited state can be analyzed as a three-exponential function.

The excimer fluorescence can be analyzed in both solvents and for each diastereomer as being composed of a double grow-in with parameters λ_F and λ_E and a decay with parameter λ_S. The parameter λ_E corresponds to the third component in the analysis of the locally excited state above −20 °C, suggesting it to be due to the excimer dissociation and locally excited-state repopulation. No change of decay parameters and of the ratio of the preexponentials was observed when analyzing the excimer emission over the whole wavelength region from 450 to 530 nm; neither was any change of the emission band shape detected by means of time-resolved fluorescence spectroscopy. These results indicate that only one excited complex geometry is formed in BPA and, as a consequence, suggest that excimer formation occurs from two ground-state conformations in a consecutive pathway.

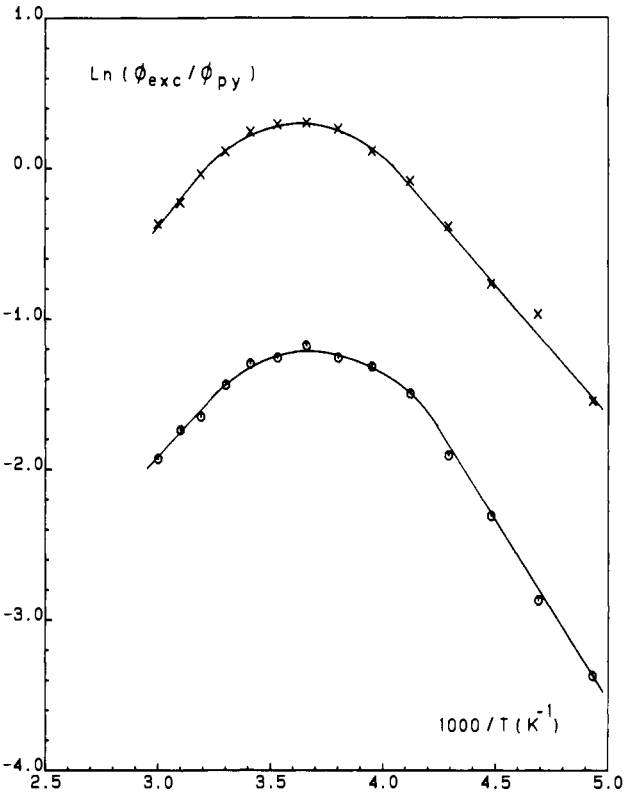

Figure 4. Natural logarithm of the ϕ_{exc}/ϕ_{py} ratio in ethyl acetate vs. 1/temperature from −70 to +60 °C: ×, e-BPA; ○, t-BPA.

Discussion

From the results presented above, it can be concluded that BPA adopts two sets of ground-state conformations in equilibrium: (1) an extended conformation with alternating side groups, also called the C_5 conformation, because of the five-membered ring with a weak hydrogen bond between the NH and CO functions of the same amino acid residue.[15] This conformation is characterized

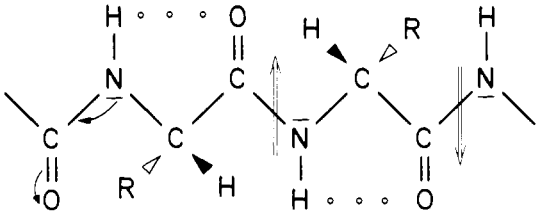

(15) Tsuboi, M.; Shimanouchi, T.; Mizushima, S. *J. Am. Chem. Soc.* **1959**, *81*, 1406–1411.

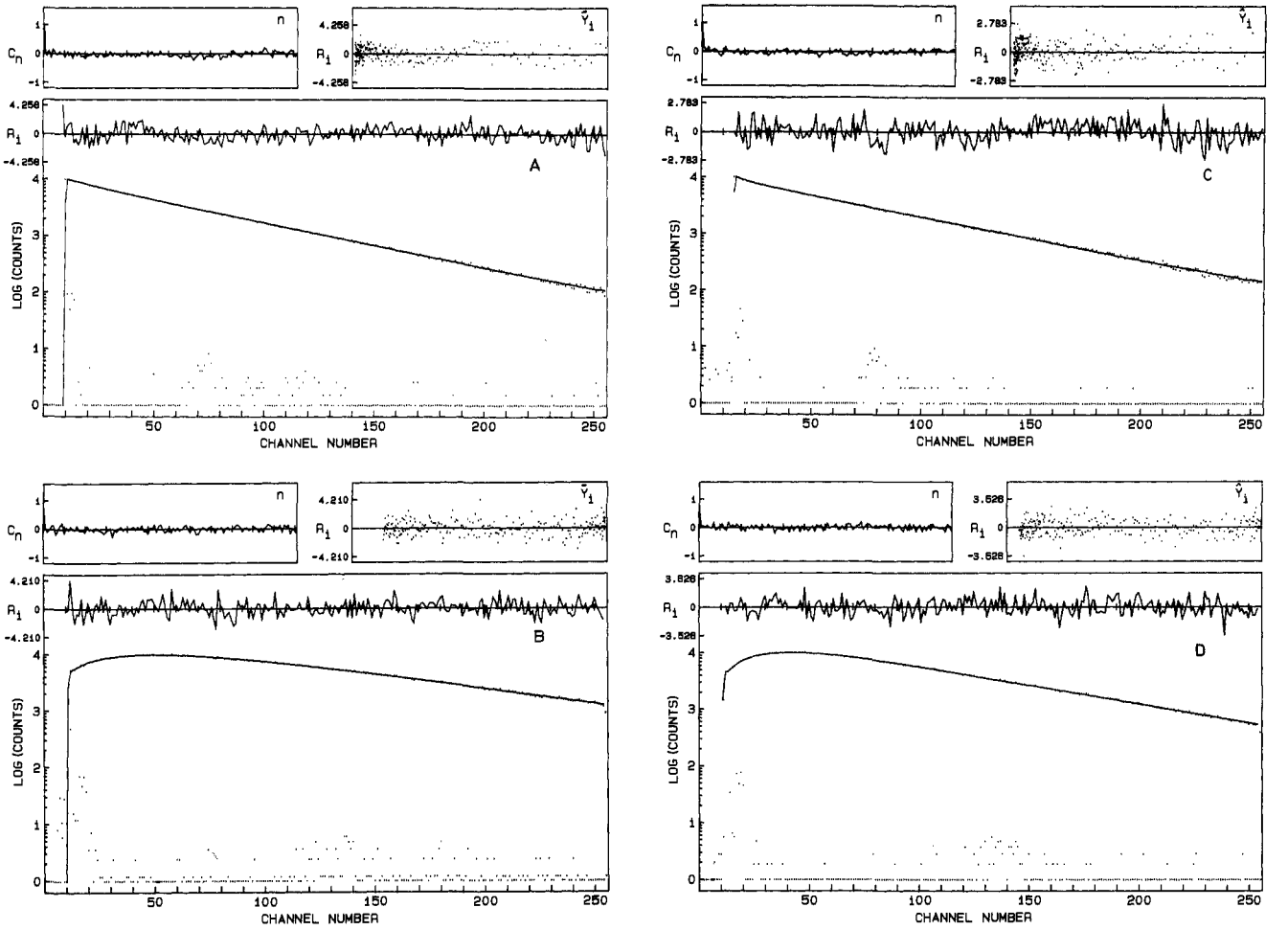

Figure 5. Experimental decay curves, instrumental response function, and calculated decay curves of BPA in ethyl acetate: (A) t-BPA, locally excited state (χ^2 = 1.11, Durbin–Watson parameter = 1.61); (B) t-BPA, excimer (χ^2 = 0.99, Durbin–Watson parameter = 1.89); (C) e-BPA, locally excited state (χ^2 = 0.99, Durbin–Watson parameter = 1.75); (D) e-BPA excimer (χ^2 = 1.24, Durbin–Watson parameter = 1.97).

by some other stabilizing phenomena prohibiting the side groups from approaching each other: all-trans chain configuration resulting in an antiparallel orientation of the peptide dipoles and the semi-double-bond character of the peptide function due to amide resonance. As a consequence, this C_5 conformation does not allow a transition to an excimer geometry, within the lifetime of excited pyrene.

(2) The other set is a folded conformation, C_7, supported by an intramolecular hydrogen bond, with the pyrenyl side groups orientated at the same side of the molecule. This C_7 conformation can be present in two configurations: axial (C_7^{ax}) and equatorial (C_7^{eq}) (Figure 6), the equilibrium between both conformers being characterized by a transition rate even higher than in the cyclohexane molecule. As a result, the single photon counting apparatus cannot distinguish between both species and detects an intermediate decay of a time-averaged C_7 conformation.[16] The component decaying slowly with parameter λ_S is ascribed to the decay of the extended conformation and the component with parameter λ_F to the decay of the folded conformation.

From intensive IR and ^{1}H NMR studies, Cung et al. concluded that other conformations in such dipeptides are adopted only at very high temperatures.[17] This interpretation of the experimental data is supported by an infrared analysis of t- and e-BPA in acetonitrile; two bands in the NH absorption region are observed, at 3420 and 3350 cm^{-1}. These bands are also reported in the spectra of the *N*-acetyl-*N'*-methylamides of several other amino acids,[18] the former being ascribed to the C_5 and the latter to the

Scheme I

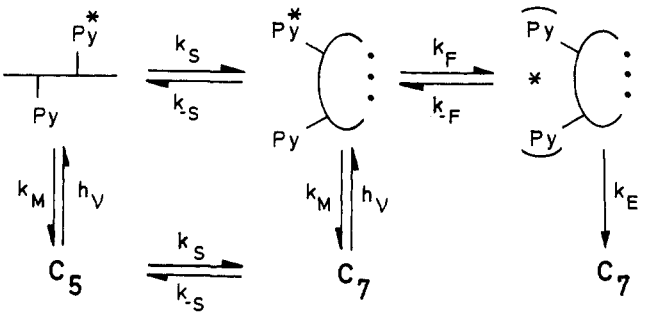

with $k_M = k_{FM} + k_{IM}$

$k_E = k_{FE} + k_{IE}$

C_7 conformation. This C_7 absorption band was absent in the infrared spectrum of PA, lacking an amide NH in the carboxylate protecting group.

As a consequence, the consecutive kinetic scheme in Scheme I describes the excimer formation in e- and t-BPA. k_S and k_F are the rate constants of the extended conformation $C_5(S)$ folding to $C_7(F)$ and of forming the excimer out of the folded conformation, respectively. The reverse processes are symbolized by

(16) In the remaining part of the paper the symbol C_7 will denote the time-averaged equilibrium between C_7^{ax} and C_7^{eq}.

(17) Cung, M. T.; Marrand, M.; Néel, *Ann. Chim. (Paris)* **1972**, *7*, 183–209.

(18) (a) Toniolo, C. *CRC Crit. Rev. Biochem.* **1980**, 5–7. (b) Mizushima, S.; Shimanouchi, T.; Tsuboi, M.; Suglta, T.; Kurosaki, K.; Mataga, N.; Souda, R. *J. Am. Chem. Soc.* **1952**, *74*, 4639–4641. (c) Avignon, M.; Huong, P. V.; Lascombe, J.; Marraud, M.; Néel, J. *Biopolymers* **1969**, *8*, 69–89. (d) Maxfield, F. R.; Leach, S. J.; Stimpson, E. R.; Powers, S. P.; Sheraga, H. A. *Ibid.* **1979**, *18*, 2507–2521. (e) Rao, C. P.; Balaram, P.; Rao, C.N.R. *Ibid.* **1983**, *22*, 2091–2104.

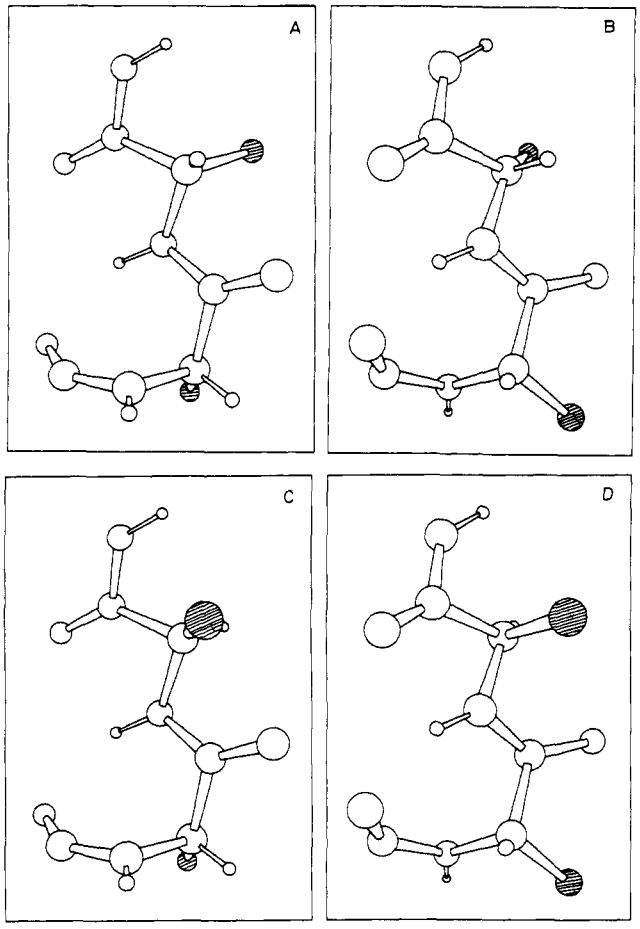

Figure 6. Conformational plots of (A) t-C_7^{ax}, (B) t-C_7^{eq}, (C) e-C_7^{ax}, and (D) e-C_7^{eq} of a dipeptide chain fragment. For simplicity, the side groups are depicted by the shaded circles.

k_{-S} and k_{-F}. k_{FM} and k_{FE} are the rate constants of the radiative decay of respectively the locally excited state and the excimer, and k_{IM} and k_{IE} symbolize the radiationless decay of both species. In this kinetic scheme, it is assumed that the conformational transitions in the ground state are described by the same rate constants as in the excited state.

The diastereomeric difference in the spectral (lower ϕ_{exc}/ϕ_{py} of t-BPA) and the transient behavior (lower A_F/A_S ratio of t-BPA) can be explained in terms of different conformational populations of both diastereomers due to the orientation of the amino acid side groups. Figure 6 illustrates the severe steric hindrance between the pyrenyl side groups of t-C_7; this steric hindrance is significantly less in e-C_7,[19] suggesting a higher C_7 population in the erythro diastereomer and, as a result, a higher probability of excimer formation. Recent theoretical calculations on both diastereomers of the Ala–Ala dipeptide show also a significant lower folding probability for the threo sequence.[20] The solvent influence on the ϕ_{exc}/ϕ_{py} and the A_F/A_S ratios arises from similar effects: in toluene, a high C_7 population is present, the molecule being stabilized by the intramolecular hydrogen bond. Addition of hydrogen acceptors such as ethyl acetate destroys this hydrogen bond and shifts the equilibrium toward the C_5 conformation, being stabilized by hydrogen bonds with the solvent.

Of course, alcohols also shift the equilibrium toward C_5, but, nevertheless, these solvents can increase the ϕ_{exc}/ϕ_{py} ratio because of their hydrogen-donating properties; in very acid alcohols, the amide resonance of the peptide function is decreased by >HN|. . .HO–R interaction. As a result, the peptide function has almost a single-bond character in these solvents, creating a more flexible chain and consequently a higher probability of excimer formation.

(19) t-C_7 and e-C_7 denote the C_7 conformation (see note 16) of t- and e-BPA, respectively.

(20) Oka, M.; Nakajima, A.; *Polym. J.* **1984**, *16*, 553–558.

Scheme II

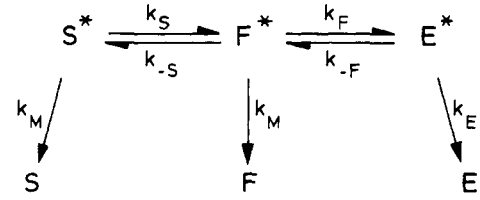

C_5 loses its stabilizing factors and rotation to an excimer geometry becomes possible. In such a case, it is tempting to compare BPA with 1,6-di(1-pyrenyl)hexane which is known to show a high ϕ_{exc}/ϕ_{py} ratio.[21]

Kinetics

A consecutive kinetic scheme was used to explain the fluorescence properties of BPA, and a more general form of it is shown in Scheme II. S* and F* are the excited states of respectively a set of conformations which first have to undergo a transition to F* to form the excimer (slow) and a set of conformations which can form the excimer independently (fast). The significance of the rate constants has been mentioned in the previous section.

In the temperature region below −20 °C, k_{-F} could be neglected. Assuming that

$$k_M = k_{FM} + k_{IM} \quad (1)$$

$$k_E = k_{FE} + k_{IE} \quad (2)$$

$$X = k_S + k_M \quad (3)$$

$$Y = k_{-S} + k_F + k_M \quad (4)$$

and at $t = 0$

$$[S^*] = k_{-S}/(k_S + k_{-S}) \quad (5)$$

$$[F^*] = k_S/(k_S + k_{-S}) \quad (6)$$

$$[E^*] = 0 \quad (7)$$

it can be shown that the decay of [S*] and [F*] upon excitation by a δ pulse is given by:

$$\begin{bmatrix}[S^*]\\ [F^*]\end{bmatrix} = \begin{bmatrix}C_{11}\\ C_{21}\end{bmatrix} a_F \exp(-\lambda_F t) + \begin{bmatrix}C_{12}\\ C_{22}\end{bmatrix} a_S \exp(-\lambda_S t) \quad (8)$$

with

$$\lambda_{F,S} = [(X + Y) \pm \sqrt{(X - Y)^2 + 4k_S k_{-S}}]/2 \quad (9)$$

$$a_F = k_M - \lambda_S \quad (10)$$

$$a_S = \lambda_F - k_M \quad (11)$$

$$C_{ij} = \begin{bmatrix}1 & 1\\ \dfrac{X - \lambda_F}{k_{-S}} & \dfrac{X - \lambda_S}{k_{-S}}\end{bmatrix} \quad (12)$$

Since both the slow and the fast conformation contribute to the emission of the locally excited state, the decay of the fluorescence is given by:

$$I_{LE}(t) \sim (k_M - \lambda_S)\left(1 + \frac{X - \lambda_F}{k_{-S}}\right)\exp(-\lambda_F t) + (\lambda_F - k_M)\left(1 + \frac{X - \lambda_S}{k_{-S}}\right)\exp(-\lambda_S t) \quad (13)$$

The time dependence of the excimer fluorescence is given by:

$$I_{EX}(t) \sim \frac{k_F(k_M - \lambda_S)}{(k_E - \lambda_F)}\exp(-\lambda_F t) + \frac{k_F(\lambda_F - k_M)}{(k_E - \lambda_S)}\exp(-\lambda_S t) + k_F\left[\frac{(\lambda_S - k_M)}{(k_E - \lambda_F)} + \frac{(k_M - \lambda_F)}{(k_E - \lambda_S)}\right]\exp(-\lambda_E t) \quad (14)$$

(21) Zachariasse, K.; Kuhnle, W. *Z. Phys. Chem. (Wiesbaden)* **1976**, *101*, 267–276.

Table IV. Calculated Values of the Rate Constants and the Conformational Distribution of e- and t-BPA in Ethyl Acetate

	e-BPA				t-BPA			
temp (°C)	k_F (s^{-1})	k_S (s^{-1})	k_{-S} (s^{-1})	f_F/f_S	k_F (s^{-1})	k_S (s^{-1})	k_{-S} (s^{-1})	f_F/f_S
−70	6.0×10^6	1.1×10^6	1.6×10^6	0.65				
−60	9.2×10^6	1.5×10^6	2.2×10^6	0.66	3.7×10^7	1.4×10^5	7.9×10^5	0.18
−50	1.2×10^7	2.2×10^6	3.3×10^6	0.68	4.3×10^7	3.2×10^5	1.3×10^6	0.24
−40	2.0×10^7	3.2×10^6	4.6×10^6	0.70	5.7×10^7	5.3×10^5	1.8×10^6	0.30
−30	2.3×10^7	4.6×10^6	5.9×10^6	0.77	6.5×10^7	8.7×10^5	2.5×10^6	0.35
−20	3.1×10^7	5.5×10^6	7.0×10^6	0.79	8.3×10^7	1.4×10^6	3.5×10^6	0.39

Table V. Calculated Values of the Rate Constants and the Conformational Distribution of e- and t-BPA in Toluene

	e-BPA				t-BPA			
temp (°C)	k_F (s^{-1})	k_S (s^{-1})	k_{-S} (s^{-1})	f_F/f_S	k_F (s^{-1})	k_S (s^{-1})	k_{-S} (s^{-1})	f_F/f_S
−80	3.7×10^6	1.9×10^5	9.3×10^4	2.09	2.9×10^7	9.4×10^4	4.5×10^5	0.22
−70	5.6×10^6	9.6×10^5	3.6×10^5	2.63	4.1×10^7	1.8×10^5	5.6×10^5	0.32
−60	7.9×10^6	1.5×10^6	6.0×10^5	2.51	6.1×10^7	6.5×10^5	1.5×10^6	0.43
−50	1.1×10^7	2.9×10^6	1.0×10^6	2.92	7.6×10^7	1.3×10^6	2.4×10^6	0.53
−40	1.5×10^7	4.6×10^6	1.6×10^6	2.91	9.7×10^7	2.1×10^6	3.3×10^6	0.63
−30	1.8×10^7	6.9×10^6	1.8×10^6	3.78	1.3×10^8	3.2×10^6	4.6×10^6	0.70
−20	2.6×10^7	9.8×10^6	3.2×10^6	3.09	1.9×10^8	4.6×10^6	6.1×10^6	0.75

Under stationary conditions of excitation, the ratio of the quantum yield of excimer emission ϕ_{EX} and emission from the locally excited state ϕ_{LE} is given by:

$$\frac{\phi_{EX}}{\phi_{LE}} = \frac{k_{FE}k_F(k_M + 2k_S)}{k_{FM}[2k_{-F}(k_M + k_S + k_{-S}) + k_E(2k_M + 2k_S + 2k_{-S} + k_{-F})]} \quad (15)$$

If $k_{-F} << k_E$, eq 15 simplifies to:

$$\frac{\phi_{EX}}{\phi_{LE}} = \frac{k_{FE}k_F(k_M + 2k_S)}{k_{FM}k_E(2k_M + 2k_S + 2k_{-S} + k_F)} \quad (16)$$

and if $k_{-F} >> k_E$ to:

$$\frac{\phi_{EX}}{\phi_{LE}} = \frac{k_{FE}k_F(k_M + 2k_S)}{2k_{FM}k_{-F}(k_M + k_S + k_{-S})} \quad (17)$$

From a measurement of τ^0, the lifetime of the unquenched chromophore (PA as reference compound), λ_S, λ_F, and A, the ratio of the preexponentials of the fast and the slow decay, all the rate constants and the conformational distribution f_F and f_S can be calculated from the following equations:

$$k_F = \lambda_F + \lambda_S - 2k_M - N_1 \quad (18)$$

$$k_S = (N_1 - N_2)/2 \quad (19)$$

$$k_{-S} = (N_1 + N_2)/2 \quad (20)$$

$$k_M = 1/\tau^0 \quad (21)$$

$$k_E = \lambda_E \quad (22)$$

$$k_{FM} = \phi^0 k_M \quad (23)$$

$$k_{IM} = k_M - k_{FM} \quad (24)$$

$$k_{FE} = \phi_E k_E \quad (25)$$

$$k_{IE} = k_E - k_{FE} \quad (26)$$

$$f_F = k_S/(k_S + k_{-S}) \quad (27)$$

$$f_S = 1 - f_F \quad (28)$$

with

$$N_1 = [C\lambda_S - \lambda_F - (C - 1)k_M]/(C - 1) \quad (29)$$

$$N_2 = [(\lambda_F - \lambda_S)^2 - N_1^2 - k_F^2]/2k_F \quad (30)$$

$$C = A(\lambda_F - k_M)/(k_M - \lambda_S) \quad (31)$$

ϕ^0 is the emission quantum yield of the unquenched chromophore.

Table VI. Preexponentials k^0_i and Activation Energies E^a_i of the Rate Constants in Tables IV and V and Enthalpy and Entropy Change of the Folding Process from C_5 to C_7

	e-EBPA (EtOAc)	t-EBPA (EtOAc)	e-EBPA (toluene)	t-EBPA (toluene)
k^0_S, s^{-1}	6.3×10^9	1.9×10^{11}	1.7×10^{11}	4.3×10^{11}
E^a_S, kcal/mol	3.5	5.9	4.8	5.7
k^0_{-S}, s^{-1}	3.5×10^9	7.1×10^9	1.5×10^{10}	1.8×10^{10}
E^a_{-S}, kcal/mol	3.1	3.8	4.2	4.0
k^0_F, s^{-1}	2.5×10^{10}	6.1×10^9	1.5×10^{10}	6.1×10^{10}
E^a_F, kcal/mol	3.4	2.1	3.1	3.0
ΔH_{fold}, kcal/mol	0.4	2.1	0.6	1.7
ΔS_{fold}, cal/mol·K	1	6	5	7

By application of eq 18–31 to the decay parameters of e- and t-BPA, the kinetic data listed in Table IV and V are obtained. In both solvents and at all temperatures, k_F of t-BPA is larger than the corresponding value of e BPA, reflecting the shorter interchromophore distance in t-C_7. It can be concluded that the higher ϕ_{exc}/ϕ_{py} ratio of e-BPA is due to the difference in C_7 population f_F, being much lower in t-BPA. This conformational effect is of greater importance than the larger k_F value of t-BPA. The values of f_F/f_S in both solvents illustrate the shift in conformational equilibrium when changing from toluene to ethyl acetate.

In Table VI the kinetic and thermodynamic parameters of the equilibrium constant $K = f_F/f_S$ of e- and t-BPA in both solvents are reported. The steric hindrance between the pyrenyl side groups in t-C_7 is depicted by the larger activation energy of folding, the lower activation energy of excimer formation, and the larger enthalpy change on folding of t-BPA, compared with the values of e-BPA.

The entropy and enthalpy changes on folding are positive for each diasteromer, indicating that the extended conformation has lower enthalpy and entropy than the folded conformation. Three stabilizing factors, limiting the mobility of C_5 and thereby lowering its entropy, were already mentioned before. In addition, the following aspects having a similar effect should be considered: (1) The solvent molecules are organized around the dipeptide by NH···OC and NH···O hydrogen bonds (ethyl acetate) and NH···π interactions (toluene). It is clear that C_5 should be more apt to perform this structuring of the solvent than C_7.

(2) In the C_5 conformation, the mobility of the pyrenyl groups is diminished by intramolecular NH (main chain)···π(side group) interactions. Since both pyrenyl groups include most of the molecular matter of BPA, the contribution of the side groups to the total entropy of the molecule should be very large. Such dipole–induced dipole interactions have been observed in peptides, composed of natural aromatic amino acids. IR and ^{1}H NMR experiments in solvents of low polarity have shown that in phe-

nylalanine peptides extended structures are preferentially stabilized over folded structures owing to the intramolecular NH···phenyl ring interactions.[22]

It should be noted that in previous studies of the folding process of natural amino acids as a function of temperature a decrease of the equilibrium constant $K = f_F/f_S$ was observed, resulting in a negative enthalpy change[23,24] and a negative entropy change.[24] However, those measurements were performed on amino acids with an aliphatic side chain (unable to interact with the peptide function) and in carbon tetrachloride or chloroform as solvent.

Conclusion

In this study, it has been shown that the molecular dynamics of the peptide chain can be probed by the excimer formation between chromophores that are covalently bound to the amino acid side chain. Both configurational and conformational effects have to be taken into account when analyzing the fluorescence decay of BPA. Two sets of ground-state conformations are important in BPA: an extended C_5 conformation which has to fold to a C_7 conformation to form the excimer and the C_7 conformation itself.

Both the ϕ_{exc}/ϕ_{py} ratio and the values of f_F/f_S, calculated from the transient measurements, indicate the ground-state conformational equilibrium shift when changing from a solvent, unable to form hydrogen bonds with the peptide function, to a solvent which destroys the intramolecular hydrogen bond of the folded conformation.

Since the enthalpy change of folding is about zero for e- and slightly positive for t-BPA, it can be concluded that the folding process is entropy driven, due to the NH···π interactions in C_5 between the chromophores and the peptide function. The diastereomeric difference, however, is due to enthalpic effects, because of the steric hindrance in t-C_7.

Acknowledgment. The authors are indebted to the University Research Fund, the FKFO, the IWONL and the NFWO for the financial support of the laboratory and to the latter for a fellowship to R.G. and M.vd.A. We thank Dr. Sisido for sending enantiomeric pure pyrenylalanine and communicating the procedure for the optical resolution of pyrenylalanine. Dr. N. Boens is thanked for developing the computer program which performs the deconvolution procedure.

Registry No. BPA (isomer 1), 91985-36-3; BPA (isomer 2), 91985-35-2.

(22) (a) Cung, M. T.; Marraud, M.; Néel, J. "Conformation of Biological Molecules and Polymers"; Bergmann, E. D., Pullman, B., Eds., *Academic* Press: New York, 1973; pp 69. (b) Toniolo, C.; Bonora, G. M.; Palumbo, M.; Peggion, E.; Stevens, E. S. *Biopolymers* **1978**, *17*, 1713-1726.
(23) Mizushima, S.; Shimanouchi, T.; Tsuboi, M.; Arakawa, T. *J. Am. Chem. Soc.* **1957**, *79*, 5357-5361.
(24) Portnova, S. L.; Bystrov, V. F.; Tsetlin, V. I.; Ivanov, V. T.; Ovchinnikov, Yu.A. *Zh. Obshch. Khim.* **1968**, *38*, 428-439.

Molecular Structure of 1,4,5,8-Tetramethylnaphthalene and In-Plane Molecular Rotation of Some Methyl-Substituted Naphthalenes in Solids

Fumio Imashiro,*[1a] Kiyonori Takegoshi,[1a] A. Saika,*[1a] Zenei Taira,[1b] and Yutaka Asahi[1b]

Contribution from the Department of Chemistry, Kyoto University, Kyoto 606, Japan, and Faculty of Pharmaceutical Sciences, Tokushima Bunri University, Tokushima 770, Japan.
Received October 9, 1984

Abstract: The crystal structure of 1,4,5,8-tetramethylnaphthalene (**1**) was determined by X-ray crystallography. Least-squares refinement of 904 independent reflections reduces to $R = 0.0609$ and $R_w = 0.0548$ ($w = 1.0$). Crystals of **1** are monoclinic, space group $P2_1/n$, $Z = 2$, $a = 7.948$ (2) Å, $b = 5.190$ (3) Å, $c = 12.887$ (2) Å, $\beta = 104.95$ (2)°. The carbon framework is nearly planar, and the adjacent peri-methyl groups take a clashed-gear conformation. The observed bond lengths and bond angles are well reproduced by molecular mechanics (MMPI) calculations on the assumption of D_{2h} symmetry for the molecular structure. Potential energy calculations for the in-plane molecular rotation of **1** in the crystalline state indicate the molecular motion in the high-temperature region is in-plane 180° flipping. The calculated barrier height (16.9 kcal mol^{-1}) compares favorably with the experimental value. In-plane molecular rotation in the solid state is also investigated for related compounds: naphthalene and 1,5- and 1,8-dimethylnaphthalenes.

How and to what extent aromatic rings keep their planarity with an increase of numbers and/or bulkiness of substituents have been of continuous interest. Recently, we deduced the planarity of methyl-substituted aromatic molecules possessing three fused rings from the barriers to rotation of their methyl groups and their ^{13}C cross-polarization–magic angle sample spinning (CPMAS) NMR spectra.[2] Several X-ray and/or neutron diffraction studies have been performed for dimethylnaphthalenes; carbon frameworks of 1,5-dimethylnaphthalene (**3**),[3] 2,6-dimethylnaphthalene,[4] and 1,8-dimethylnaphthalene (**4**)[5] are planar, whereas the carbon atoms in 3-bromo-1,8-dimethylnaphthalene (**5**)[6] are not coplanar, and further the aromatic and methyl carbon atoms in 1,8-dimethyl-2-naphthyl acetate (**6**)[7] take a "chair-like" conformation: the C1 and C5 carbons are located above the average molecular plane and the C4 and C8 carbons are located below the plane. Octamethylnaphthalene (**7**)[8,9] has a definite "chair-like" conformation; the displacement of the peri-methyl carbons is as large as 0.73 Å. "Chair-like" conformations are also observed for fully peri-halogenated naphthalenes such as 1,4,5,8-tetrachloro-

(1) (a) Kyoto University. (b) Tokushima Bunri University.
(2) Takegoshi, K.; Imashiro, F.; Terao, T.; Saika, A. *J. Chem. Phys.* **1984**, *80*, 1089-1094.
(3) (a) Beintema, J. *Acta Crystallogr.* **1965**, *18*, 647-654. (b) Ferraris, G.; Jones, D. W.; Yerkess, J.; Bartle, K. D. *J. Chem. Soc., Perkin Trans. 2* **1972**, 1628-1632.
(4) Kitaigorodskii, A. I. *Bull. Acad. Sci. URSS, Cl. Sci. Chim.* **1946**, 587-600; *Chem. Abstr.* **1948**, *42*, 7595-7596.
(5) Bright, D.; Maxwell, I. E.; de Boer, J. *J. Chem. Soc., Perkin Trans. 2* **1973**, 2101-2105.
(6) Jameson, M. B.; Penfold, B. R. *J. Chem. Soc.* **1965**, 528-536.
(7) White, D. N. J.; Carnduff, J.; Guy, M. H. P.; Bovill, M. J. *Acta Crystallogr.* **1977**, *B33*, 2986-2988.
(8) Donaldson, D. M.; Robertson, J. M. *J. Chem. Soc.* **1953**, 17-24.
(9) Sim, G. A. *Acta Crystallogr.* **1982**, *B38*, 623-625.

0002-7863/85/1507-2341$01.50/0